# Stimulated Emission of Signal Photons from Dark Matter Waves

Ankur Agrawal,[1,2,3,*] Akash V. Dixit,[1,2,3,†] Tanay Roy,[1,2,‡] Srivatsan Chakram,[1,2,4,§] Kevin He,[1,2] Ravi K. Naik,[5] David I. Schuster,[1,2,6,7] and Aaron Chou[8]

[1]James Franck Institute, University of Chicago, Chicago, Illinois 60637, USA
[2]Department of Physics, University of Chicago, Chicago, Illinois 60637, USA
[3]Kavli Institute for Cosmological Physics, University of Chicago, Chicago, Illinois 60637, USA
[4]Department of Physics and Astronomy, Rutgers University, Piscataway, New Jersey 08854, USA
[5]Computational Research Division, Lawrence Berkeley National Laboratory, Berkeley, California 94720, USA
[6]Pritzker School of Molecular Engineering, University of Chicago, Chicago, Illinois 60637, USA
[7]Department of Applied Physics, Stanford University, Stanford, California 94305, USA
[8]Fermi National Accelerator Laboratory, Batavia, Illinois 60510, USA

(Received 17 July 2023; accepted 26 January 2024; published 3 April 2024)

The manipulation of quantum states of light has resulted in significant advancements in both dark matter searches and gravitational wave detectors. Current dark matter searches operating in the microwave frequency range use nearly quantum-limited amplifiers. Future high frequency searches will use photon counting techniques to evade the standard quantum limit. We present a signal enhancement technique that utilizes a superconducting qubit to prepare a superconducting microwave cavity in a nonclassical Fock state and stimulate the emission of a photon from a dark matter wave. By initializing the cavity in an $|n = 4\rangle$ Fock state, we demonstrate a quantum enhancement technique that increases the signal photon rate and hence also the dark matter scan rate each by a factor of 2.78. Using this technique, we conduct a dark photon search in a band around 5.965 GHz (24.67 μeV), where the kinetic mixing angle $\epsilon \geq 4.35 \times 10^{-13}$ is excluded at the 90% confidence level.

DOI: 10.1103/PhysRevLett.132.140801

*Introduction.*—The existence of dark matter (DM) is one of the greatest mysteries in physics, which has puzzled scientists for nearly a century. Despite the lack of direct detection, there is compelling evidence for its existence, including its estimated contribution of 27% to the Universe's energy density and its gravitational effects on galaxy dynamics and structure formation [1–3]. Axions and dark photons have emerged as leading candidates for dark matter due to their cosmological origins and low-energy properties, which allow them to exist as coherent waves with macroscopic occupation numbers [4–8]. Dark matter haloscope experiments in the microwave frequency range use a cavity to resonantly enhance the oscillating electric field generated by the DM field at a frequency corresponding to the mass of a hypothetical particle ($\nu = mc^2/h$) [8,9]. Since the mass of DM is unknown *a priori*, experimental searches are typically conducted as radio scans in which the resonant cavity is tuned one step $d\nu$ at a time to test different frequency hypotheses. A key figure of merit is therefore the frequency scan speed, which in a photon counting experiment scales as $d\nu/dt \propto d\nu R_s^2/R_b$ where $R_s$ and $R_b$ are the signal and background count rates, respectively.

Quantum techniques have proven useful in accelerating the scan rate of axion and wavelike dark matter searches [10–12]. Superconducting parametric amplifiers, which are quantum-limited, have reached the standard quantum limit (SQL) and add only $1/2$ photon of noise per mode, as required by the Heisenberg uncertainty principle for phase-preserving measurements [13–17]. Alternatively, qubit-based single photon detection [18] does not consider the photon phase and can, in principle, measure without any added detection noise by achieving extremely low, sub-SQL background rates.

While both of these methods employ quantum technologies, their operation is in some sense recognizable as an ideal classical amplifier and microwave photomultiplier. Parametric amplifiers and cavity-qubit systems can also synthesize inherently quantum mechanical states of light such as squeezed states [19–21] in the former and Fock states [22,23] or cat states [24–28] for the latter. Recently, squeezed state injection paired with phase-sensitive amplification was used to improve the scan rate of the HAYSTAC experiment [29]. In this work, we develop a new method in which we prepare an $n$-photon Fock state which enhances the signal rate by $\eta(n + 1)$ times where $\eta$ is the efficiency of

detecting the state. By creating a Fock state with $|n=4\rangle$ photons in the cavity, we observe a 2.78-fold enhancement in the signal rate. We show that this technique is compatible with the previously demonstrated noise reduction from photon counting [18].

The power delivered to the cavity by a current density generated by dark matter $\mathbf{J}_{\mathrm{DM}}$ is given by $P_s = \int dV \mathbf{J}_{\mathrm{DM}}(x) \cdot \mathbf{E}(x)$, which is proportional to the magnitude of oscillating electric field $\mathbf{E}(x)$ in the cavity. In the conventional scenario, the cavity is cooled to the vacuum state, and the signal electric field builds up monotonically over the coherence time of the cavity or of the dark matter wave in a process akin to spontaneous emission. Alternatively, we may initialize the cavity with a nonzero $\mathbf{E}(x)$ field from a coherent state or from a Fock state to induce stimulated emission. The Fock state has some advantages. First, unlike the homodyne or heterodyne detection using a coherent state pump, the Fock state is free from any shot noise, making it possible to measure small signal amplitudes far below the SQL. Second, a Fock state is symmetric in phase, making it equally sensitive to any instantaneous phase of the incoming DM wave, which is unknown *a priori*.

We can model the action of the DM wave on a Fock state as a classical drive amplitude $\xi$ which shifts this phase-symmetric state away from the origin in the Wigner phase space by $\alpha$ (see Supplemental Material [30], Fig. S1 which includes Refs. [31,32]). The resultant state comprises both in-phase components which extracted excess power from the DM wave and also out-of-phase components which delivered their power to the DM wave. The stimulated emission process for DM converting into photons is enhanced by a factor of $(n+1)$, while the stimulated absorption process is enhanced by a factor of $n$. Mathematically, the stimulated emission into the cavity state from a dark matter wave can be described as shown:

$$|\langle n+1|\hat{\mathcal{D}}(\alpha)|n\rangle|^2 = |\langle n+1|e^{(\alpha a^\dagger - \alpha^* a)}|n\rangle|^2 \sim |\langle n+1|\alpha a^\dagger|n\rangle|^2 = (n+1)\alpha^2, \quad (1)$$

where $\hat{\mathcal{D}}(\alpha)$ is the displacement operator. From Eq. (1), we can infer that the displacement ($\alpha \ll 1$) induced by the DM wave on a cavity prepared in $|n\rangle$ Fock state results in population of $|n+1\rangle$ state with probability proportional to $(n+1)$. Using number-resolving measurements, the signal can thus be observed with $(n+1)$ times greater probability.

We note that just as in other cases of quantum-enhanced metrology, the $(n+1)$ enhancement factor in the signal transition probability can be exactly canceled by the $1/(n+1)$ reduction in the coherence time of the probe. As a result, there would be no net improvement in the actual signal rate $R_s$. However, this consideration does not apply when the limiting coherence time is that of the dark matter wave rather than of the Fock photon state in the cavity. In such cases, the signal rate is not degraded by the reduction of the probe coherence time and retains the factor $(n+1)$. To our knowledge, this is one of the few cases where quantum metrology can provide a realizable improvement in a real-world application. Also, since the readout rate scales as the inverse of the probe coherence time, the background count rate may also scale linearly with $(n+1)$, for example, for backgrounds associated with readout errors. For experiments with fixed tuning step size $d\nu$ given, for example, by the dark matter linewidth, the improvement in scan speed $d\nu/dt \propto d\nu R_s^2/R_b$ is therefore a single factor of $\eta(n+1)$.

*Fock state preparation and photon number resolving detector.*—We couple the cavity to a nonlinear element, in this case a superconducting transmon qubit to prepare and measure the Fock states, which are otherwise impossible to create in a linear system such as a cavity. The device used in this work is composed of three components—a high quality factor ($Q_s = 4.06 \times 10^7$) 3D multimode cavity [33] to accumulate and store the signal induced by the dark matter (storage, $\omega_s/2\pi = 5.965$ GHz), a superconducting transmon qubit ($\omega_q/2\pi = 4.95$ GHz), and a 3D cavity strongly coupled to a transmission line ($Q_r = 9 \times 10^3$) used to quickly read out the state of qubit (readout, $\omega_r/2\pi = 7.789$ GHz) [Fig. 1(a)]. We mount the device to the base stage of a dilution refrigerator operating at 10 mK.

The interaction between a superconducting transmon qubit [35,36] and the field in a microwave cavity is described by the Jaynes-Cummings Hamiltonian [37] in the dispersive limit (qubit-cavity coupling $\ll$ qubit-cavity detuning) as

$$\mathcal{H}/\hbar = \omega_s a^\dagger a + \frac{1}{2}(\omega_q + \chi a^\dagger a)\sigma_z, \quad (2)$$

where $a$ ($a^\dagger$) is the annihilation (creation) operator of the cavity mode and $\sigma_z$ is the Pauli $Z$ operator of the transmon. Equation (2) elucidates a key feature of this interaction—a photon number dependent shift ($\chi$) of the qubit transition frequency [see Fig. 1(b)] [38]. Another important feature of this Hamiltonian is the quantum nondemolition (QND) nature of the interaction between the qubit and cavity which preserves the cavity state upon the measurement of the qubit state and vice versa [38–40]. By driving the qubit at the Stark shifted frequency $(\omega_q + n\chi)$, one would selectively excite the qubit if and only if there are exactly $n$ photons in the cavity.

Recent works have shown that a single transmon has the capability to prepare any quantum state in a cavity and perform universal control on it [21,25,41–44]. In this study, we used a gradient ascent pulse engineering (GRAPE) based method to generate optimal control pulses (OCT) [25,45] that consider the full model of the time-dependent Hamiltonian and allow us to prepare nonclassical states in a cavity. As shown in Fig. 1(b), our approach successfully prepared cavity Fock states with pulse duration as short as $\mathcal{O}(1/\chi)$, which did not increase for higher Fock states.

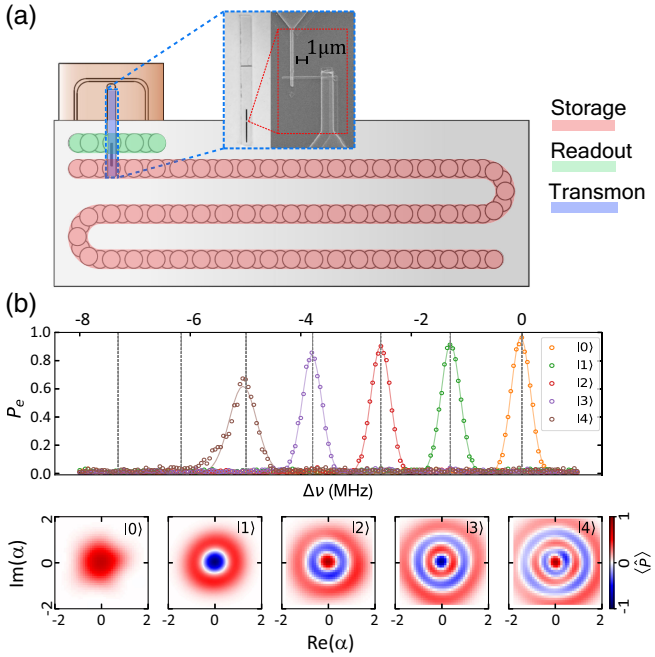


FIG. 1. Fock state preparation in a cavity dispersively coupled to a transmon qubit. (a) A schematic of the multimode flute cavity showing the location of the storage cavity (red), readout cavity (green), and transmon chip (blue) with an SEM image of the Josephson junction (see cavity fabrication and surface preparation in [33]). (b) Fock states with up to $n = 4$ are created using GRAPE method and characterized by measuring qubit spectroscopy (top) and Wigner tomography (bottom) [34]. Successful Fock state generation is evident from single peaks in spectroscopy and alternating negative and positive rings in the tomography (see Supplemental Material [30] Sec. D for details).

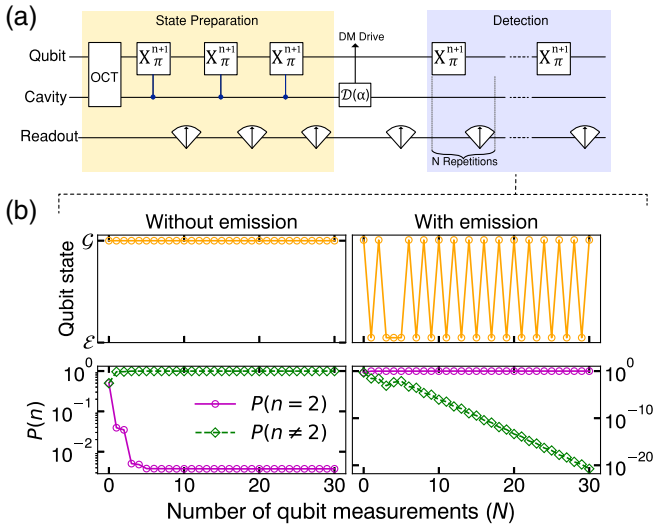


FIG. 2. Stimulated emission protocol with number resolved $\pi$ pulse and hidden Markov model analysis. (a) Pulse sequence for stimulated emission includes cavity initialization in a Fock state, followed by three conditional checks to ensure the cavity did not accidentally start in $|n+1\rangle$ state. The next part involves a cavity displacement drive to mimic an interaction with DM, and repeated conditional qubit measurements to detect the cavity in $|n+1\rangle$ state. (b) Examples showing two measured qubit readout sequences for a cavity initialized in $|n\rangle = 1$ Fock state followed by a small displacement drive $\alpha$. The left panel corresponds to no change in the cavity state after the DM drive as inferred by the absence of successful flips of the qubit state which results in a very small probability $P(n = 2)$ that the cavity was in the $|n = 2\rangle$ Fock state. The right panel corresponds to an emission event where the cavity state changed from $|1\rangle \rightarrow |2\rangle$, resulting in multiple successful flips of the qubit state. Even with a potential readout error in the 5th measurement, the HMM analysis of this sequence of flips then indicates a very high likelihood ratio to be in $|n = 2\rangle$ Fock state. We observe an exponential suppression of the detector-error induced false positive probability with only linear increase in the number of repeated measurements.

*Stimulated emission protocol.*—The stimulated emission protocol is divided into two parts: the first part involves the preparation of cavity in a desired Fock state, $|n\rangle$ and the second part involves the detection of the cavity in the $|n+1\rangle$ Fock state as depicted in Fig. 2(a). In order to actively suppress any false positive events such as the cavity accidentally starting in $|n+1\rangle$ state, we conditionally excite the qubit with a number resolved $\pi$ pulse at the $(n+1)$-shifted peak 3 times. If and only if the qubit fails to excite in all three attempts do we proceed ahead with the rest of the protocol. By doing this, we can suppress the false positive rate $\leq 3\%$.

At the end of this sequence, we measure the efficiency of the state preparation for each $n$ by measuring the qubit excitation probability $P_n$ with a number resolved $\pi$ pulse centered at the $|n\rangle$ peak. The measured fidelities are $P_0 = 95.2 \pm 0.3\%$, $P_1 = 91.2 \pm 0.4\%$, $P_2 = 87.3 \pm 0.5\%$, $P_3 = 81.6 \pm 0.6\%$, $P_4 = 63.6 \pm 0.7\%$ [see Fig. 1(b) top panel].

After the state preparation, we apply a coherent drive to the cavity mimicking an interaction with the DM wave to characterize the detector. A series of repeated QND measurements are recorded by performing conditional $\pi$ pulses centered at the $(n+1)$-shifted peak. The time between two successive QND measurements is 5 μs, which is relatively short compared to the lifetime of $|n\rangle$ given by $T_1^s = 1320\ \mu\text{s}/n$ (see Table S1 [30]). This projective measurement resets the clock on the decay of the $|n+1\rangle$ state [46]. We then apply a hidden Markov model (HMM) analysis to reconstruct the cavity state and compute the probability that the cavity state had changed from $|n\rangle \rightarrow |n+1\rangle$ and assign a likelihood ratio $\lambda$ associated with such events (see Supplemental Material [30], Sec. G for implementation of HMM analysis which includes Ref. [47]).

In principle, it is possible to prepare Fock states $|n > 4\rangle$ in the device. However, due to the presence of multiple cavity modes, simulating the complete Hamiltonian to generate the OCT pulses becomes computationally challenging and in practice, higher $(n+1)$ Fock states are prepared with lower fidelity. Furthermore, to prevent excessive signal photon loss, the Fock state decay rate

which is also enhanced by a factor of $(n+1)$ must remain small compared to the sum of Stark shift and readout rate, which determines the maximum rate of number resolved measurements. For this study, we chose $|n=4\rangle$, such that the decay probability stays below 1% between successive measurements.

*Signature of Fock enhancement.*—To assess the performance of the detector after preparing the cavity in a particular Fock state $|n\rangle$, we carry out a series of experiments. We apply a small variable displacement ($\alpha \ll 1$) to the cavity and measure the relationship between the number of injected ($n_{\mathrm{inj}} = |\alpha|^2$) and detected photons. We perform 30 repetitions of the qubit measurement and apply a likelihood threshold of $\lambda_{\mathrm{thresh}} = 10^3$ to distinguish positive and negative events. This threshold is determined based on the background cavity occupation $n_b^c = 6 \times 10^{-3}$, which is assumed to be caused by photon shot noise from a hot cavity, as measured using the photon counting method described in [18] (refer to Supplemental Material [30] Fig. S11). Errors below this value are considered to be subdominant. The data obtained from the characterization of the detector is fitted to an expression, represented by Eq. (3) (see Supplemental Material [30], Sec. H on detector characterization).

$$n_{\mathrm{meas}} = \eta P_{nl}(|\alpha|^2 = \bar{n}) + \delta. \tag{3}$$

When initialized in $|n\rangle$, $P_{nl}(|\alpha|^2)$ is the probability of finding the cavity in $|l\rangle$ after being displaced [48] (see Supplemental Material [30], Sec. A for details). This equation takes into account the detection efficiency, $\eta$, and false positive probability, $\delta$. In cases where the cavity displacement $\alpha \ll 1$, $P_{nl}(|\alpha^2|) \approx (n+1)|\alpha^2|$, as shown in Eq. (1).

Figure 3 displays the unique characteristic of stimulated emission enhancement, where a higher number of detected photons is observed for the cavity that was initialized in a higher Fock state. This manifests as a monotonic increase in the slope of the detected vs injected photon number relation as the initial prepared Fock number increases. This result aligns with expectations and highlights the effectiveness of stimulated emission as a method for amplifying weak signals. The resultant enhancement between $|n=4\rangle$ and $|n=0\rangle$ is 2.78 $(= 0.45 \times 5/0.81 \times 1)$. The reduced efficiency $\eta_4 = 0.45$ to see the full $(n+1)$ enhancement can be explained by the enhanced decay rate and higher demolition probability of higher Fock state (see Supplemental Material [30], Sec. H for further discussion). The false positive probabilities $\delta$ are smaller than $10^{-4}$ for all Fock states, comparable to the measured residual photon occupation in the cavity.

We observe anomalous behavior for the $|n=3\rangle$ data which shows no signal enhancement. We suspect the cause to be a leakage to a nearby mode as the cavity contains multiple modes which are closely spaced [33]. We have identified a couple of transitions with different modes that are closer in energy level with $|g,3\rangle$ and which could be facilitated by the always-on interaction of the transmon with all the modes. This frequency collision issue can be easily resolved in future designs such that the cavity modes are spaced further apart and the transmon has negligible overlap with the spectator modes.

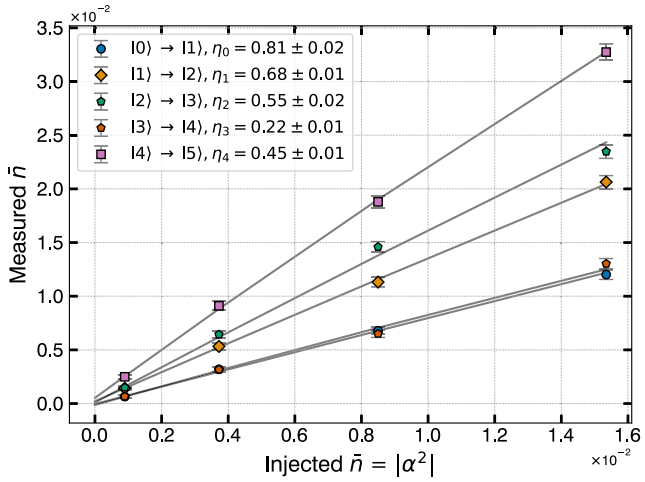


FIG. 3. Stimulated emission enhancement. Mean number of measured photons (positive events) as a function of the mean number of injected photons in the cavity. We initialize the cavity in a Fock state $|n\rangle$, apply a variable displacement, perform 30 repeated qubit measurements, and analyze the measurement sequence using the HMM technique. We choose a detection threshold ($\lambda_{\mathrm{thresh}} = 10^3$) such that the detector errors are subdominant to the residual photon ($n_b^c = 6 \times 10^{-3}$) induced false positives, $\lambda_{\mathrm{thresh}} > 1/n_b^c$ [18] and subtract background detections when no displacement ($\alpha = 0$) is applied. The monotonic decrease in the detector efficiency is attributed to higher decay probability and demolition probability at higher photon number (see Supplemental Material [30], Fig. S9 which includes Ref. [49]). Anomalous behavior in $|3\rangle$ is attributed to the state decaying to nearby modes in the band structure formed by multiple modes of the cavity, qubit, and readout, which are close in the energy level $|q,s,r\rangle$. For a particular displacement, more photons are detected for increasing photon number of the initial Fock state prepared. This is a clear signature of stimulated emission with an enhancement of $\eta_4(4+1)/\eta_0(0+1) = 2.78$ when the cavity is prepared in $|n=4\rangle$ as compared to $|n=0\rangle$.

*Dark photon search.*—In order to conduct a dark photon search, we collect independent datasets for a cavity prepared in different Fock states and count the number of positive events in the absence of the mock DM drive. Additionally, we vary the dwell time ($\tau$) between the state preparation and the beginning of the measurement sequence in order to allow the coherent buildup of cavity field due to the dark matter. Once the measurement sequence begins, the quantum Zeno effect prevents further buildup of the signal field. Ideally, one would like to choose the dwell time as close to the lifetime of Fock state as possible to maximize the accumulation of signal and thus,

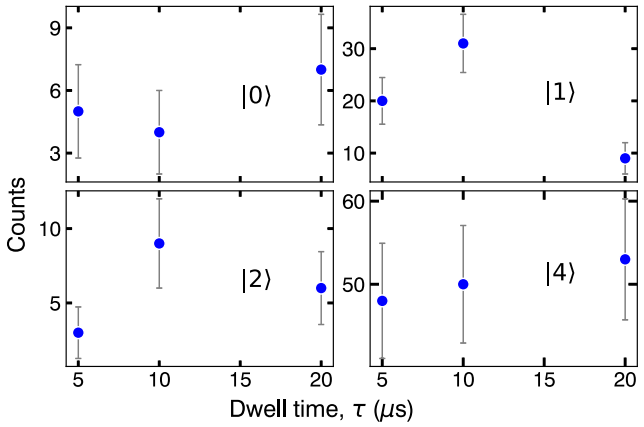


FIG. 4. Measured background counts for different Fock states in the cavity as a function of dwell time. There is no clear trend in the number of observed background counts indicating systematic effects which could be due to the state preparation steps. The error bars are plotted as $\sqrt{\text{Counts}}$ with $N_{\text{trials}} \sim 20\,000$ for each point.

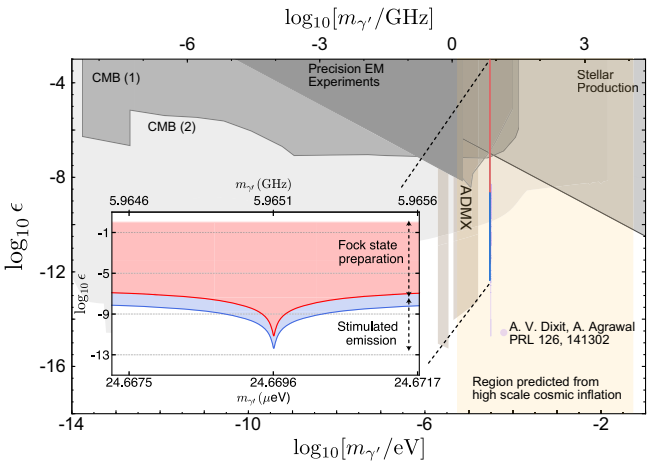


FIG. 5. Exclusion of dark photon parameter space with stimulated emission. Shaded regions in the dark photon parameter space [7,51] of coupling ($\epsilon$) and mass ($m_\gamma$) are excluded. In the orange band, dark photon is naturally produced in models of high scale cosmic inflation [8]. The exclusion set with stimulated emission based dark photon search is shown in the blue and red curves. On resonance with the storage cavity ($m_{\gamma'}c^2 = \hbar\omega_s$), the dark photon kinetic mixing angle is constrained to $\epsilon \leq 4.24 \times 10^{-13}$ with 90% confidence. (Inset) The horizontal extent of the excluded region is set by the bandwidth of the number resolved qubit $\pi$ pulse which is insensitive to any drive outside the band. The vertical limit is set by the maximum $\epsilon$ which would result in dark photon rate greater than the value which would degrade the fidelity of Fock state preparation significantly (See Supplemental Material [30], Fig. S12). The blue shaded region represents the exclusion with the stimulated emission experiment.

the scan rate. In this work, the dwell time was varied to compare on equal footing the dependence on $n$ and not optimized for DM sensitivity. For this study, we chose a maximum dwell time of 20 μs to collect reasonable statistics with $\lambda_{\text{thresh}} = 10^3$ for all Fock states. Longer integration times comparable to or larger than the dark matter coherence time (75 μs) which are needed to realize the full benefit of Fock enhancement will be implemented in future dedicated experiments.

The number of measured counts shown in Fig. 4 is fit to a functional form given by Eq. (4) (see Supplemental Material [30], Sec. J), which has contributions coming from a coherent source [hence the $(n+1)$ Fock enhancement factor], an incoherent source, and a state preparation dependent error

$$N_{\text{meas}} = a_0(n+1)\tau(N_{\text{trials}}\tau) + b(N_{\text{trials}}\tau) + c_n N_{\text{trials}}, \quad (4)$$

where $a_0$ and $b$ and $c_n$'s are the fit parameters we extract from fitting the measured counts. The first term has two factors of $\tau$: one from the coherent buildup of signal energy in the storage cavity for $\tau < T_1^s$ which is included in the average signal rate $dN/dt$, and a second factor of $\tau$ for the total integration time $t_{\text{tot}} = N_{\text{trials}}\tau$.

We extract the value of $a_0$, and compute the kinetic mixing angle of the dark photon given by $\epsilon = \sqrt{(a_0/\rho_{\text{DM}} m_{\text{DM}} GV)}$ (see Supplemental Material [30], Sec. J for fitting method and derivation). With the measured uncertainties on all the parameters and using error propagation, we compute the 90% confidence limit on $\epsilon$ to be $\epsilon_{\text{fit}} + 1.28\sigma_\epsilon$. Thus, a dark photon candidate on resonance with the storage cavity ($m_{\gamma'}c^2 = \hbar\omega_s$), with mixing angle $\epsilon \geq 4.35 \times 10^{-13}$ is excluded at the 90% confidence level. Figure 5 shows the regions of dark photon parameter space excluded by the stimulated emission based search, assuming the dark photon comprises all the dark matter density ($\rho_{\text{DM}} = 0.4\ \text{GeV/cm}^3$). The detector is maximally sensitive to dark matter candidates with masses within a narrow window around the resonance frequency of the cavity. This window is set by the lineshape of the dark matter [50] ($Q_{\text{DM}} \sim 10^6$). For DM wave at ~6 GHz, the FWHM linewidth is 6 kHz, so the −3 dB point is 3 kHz away from the cavity resonance. Additionally, sensitivity to off-resonant signals is reduced when the associated qubit Stark shift falls outside of the finite bandwidth of the $\pi$ pulses used to interrogate the qubit. While the stimulated emission protocol is valid for small induced signal, the cavity state preparation using OCT pulses excludes DM wave corresponding to $|\alpha| > 0.05$ (see Fig. S17) as it would result in larger preparation error than experimentally observed.

*Conclusions and outlook.*—The preparation of a cavity in quantum states of light, such as a Fock state, has the potential to significantly enhance the DM signal rate and hence also the DM frequency scan rate compared to previous methods. In the current work, we have demonstrated a signal enhancement of 2.78× by initializing the cavity in the $|n=4\rangle$ versus $|n=0\rangle$ Fock state and performed a dark photon search setting new limits in unexplored parameter space. In an

optimized experiment, the dead time due to state preparation and interrogation can be minimized to be comparable to other photon counting protocols. This method holds great promise for continued improvement as advancements in cavity coherence times [52] and state preparation methods [21] enable access to even larger $n$ Fock states. Unlike the present dark photon search, future axion dark matter experiments will require the target cavity to be immersed in a high magnetic field, precluding *in situ* operation of superconducting qubits. In this case, the probe state must be prepared in a remote field-free location and transferred to the target cavity. After integrating the axion interaction, the probe state can be transferred back to the remote location for measurement. An example of such a state-swapping protocol is given in [53].

While this study focuses on the detection of dark matter, the quantum-enhanced technique presented here can be applied more widely to sense ultraweak forces in various settings, in cases where the signal accumulation is limited by the coherence time of the signal rather than by that of the probe. The Fock state stimulated emission can increase the rate of processes that involve the delivery of small amounts of energy, and the resulting signal quanta can be detected through number-resolved counting techniques that surpass the SQL.

We would like to acknowledge and thank Konrad Lehnert for proposing this idea. We thank Ming Yuan, A. Oriani, and A. Eickbusch for discussions, and the Quantum Machines customer support team for help with implementing the control software. We gratefully acknowledge the support provided by the Heising-Simons Foundation. This work made use of the Pritzker Nanofabrication Facility of the Institute for Molecular Engineering at the University of Chicago, which receives support from Soft and Hybrid Nanotechnology Experimental (SHyNE) Resource (NSF ECCS-1542205), a node of the National Science Foundation's National Nanotechnology Coordinated Infrastructure. This Letter has been authored by Fermi Research Alliance, LLC under Contract No. DE-AC02-07CH11359 with the U.S. Department of Energy, Office of Science, Office of High Energy Physics, with support from its QuantISED program. We acknowledge support from the Samsung Advanced Institute of Technology Global Research Partnership.

[*]ankur.agrawal92@gmail.com
Present address: AWS Center for Quantum Networking, Boston, Massachusetts 02145, USA.
[†]Present address: National Institute of Standards and Technology, Boulder, Colorado 80305, USA.
[‡]Present address: Superconducting Quantum Materials and Systems Center, Fermi National Accelerator Laboratory, Batavia, Illinois 60510, USA.
[§]Present address: Department of Physics and Astronomy, Rutgers, the State University of New Jersey, Piscataway, New Jersey 08854, USA.

[1] Aaron S. Chou *et al.*, Snowmass cosmic frontier report, arXiv:2211.09978.
[2] M. Tanabashi, K. Hagiwara, K. Hikasa, K. Nakamura, Y. Sumino *et al.* (Particle Data Group), Review of particle physics, Phys. Rev. D **98**, 030001 (2018).
[3] V. C. Rubin, N. Thonnard, and W. K. Ford, Jr., Rotational properties of 21 SC galaxies with a large range of luminosities and radii, from NGC 4605/R = 4 kpc/ to UGC 2885/R = 122 kpc/, Astrophys. J. **238**, 471 (1980).
[4] John Preskill, Mark B. Wise, and Frank Wilczek, Cosmology of the invisible axion, Phys. Lett. **120B**, 127 (1983).
[5] L. F. Abbott and P. Sikivie, A cosmological bound on the invisible axion, Phys. Lett. **120B**, 133 (1983).
[6] Michael Dine and Willy Fischler, The not-so-harmless axion, Phys. Lett. **120B**, 137 (1983).
[7] Paola Arias, Davide Cadamuro, Mark Goodsell, Joerg Jaeckel, Javier Redondo, and Andreas Ringwald, WISPy cold dark matter, J. Cosmol. Astropart. Phys. 06 (2012) 013.
[8] Peter W. Graham, Jeremy Mardon, and Surjeet Rajendran, Vector dark matter from inflationary fluctuations, Phys. Rev. D **93**, 103520 (2016).
[9] P. Sikivie, Experimental tests of the "Invisible" axion, Phys. Rev. Lett. **51**, 1415 (1983).
[10] B. M. Brubaker, L. Zhong, Y. V. Gurevich, S. B. Cahn, S. K. Lamoreaux, M. Simanovskaia, J. R. Root, S. M. Lewis, S. Al Kenany, K. M. Backes, I. Urdinaran, N. M. Rapidis, T. M. Shokair, K. A. van Bibber, D. A. Palken, M. Malnou, W. F. Kindel, M. A. Anil, K. W. Lehnert, and G. Carosi, First results from a microwave cavity axion search at 24 μeV, Phys. Rev. Lett. **118**, 061302 (2017).
[11] T. Braine, R. Cervantes, N. Crisosto, N. Du, S. Kimes *et al.* (ADMX Collaboration), Extended search for the invisible axion with the axion dark matter experiment, Phys. Rev. Lett. **124**, 101303 (2020).
[12] Jinsu Kim *et al.*, Near-quantum-noise axion dark matter search at CAPP around 9.5 μeV, Phys. Rev. Lett. **130**, 091602 (2023).
[13] Carlton M. Caves, Quantum limits on noise in linear amplifiers, Phys. Rev. D **26**, 1817 (1982).
[14] T. Yamamoto, K. Inomata, M. Watanabe, K. Matsuba, T. Miyazaki, W. D. Oliver, Y. Nakamura, and J. S. Tsai, Flux-driven Josephson parametric amplifier, Appl. Phys. Lett. **93**, 042510 (2008).
[15] Christopher Eichler and Andreas Wallraff, Controlling the dynamic range of a Josephson parametric amplifier, Eur. Phys. J. Quantum Technol. **1**, 2 (2014).
[16] Tanay Roy, Suman Kundu, Madhavi Chand, A. M. Vadiraj, A. Ranadive, N. Nehra, Meghan P. Patankar, J. Aumentado, A. A. Clerk, and R. Vijay, Broadband parametric amplification with impedance engineering: Beyond the gain-bandwidth product, Appl. Phys. Lett. **107**, 262601 (2015).
[17] Martina Esposito *et al.*, Development and characterization of a flux-pumped lumped element Josephson parametric amplifier, EPJ Web Conf. **198**, 00008 (2019).
[18] Akash V. Dixit, Srivatsan Chakram, Kevin He, Ankur Agrawal, Ravi K. Naik, David I. Schuster, and Aaron

Chou, Searching for dark matter with a superconducting qubit, Phys. Rev. Lett. **126**, 141302 (2021).
[19] Carlton M. Caves, Quantum-mechanical noise in an interferometer, Phys. Rev. D **23**, 1693 (1981).
[20] B. J. Lawrie, P. D. Lett, A. M. Marino, and R. C. Pooser, Quantum sensing with squeezed light, ACS Photonics **6**, 1307 (2019).
[21] Alec Eickbusch, Volodymyr Sivak, Andy Z. Ding, Salvatore S. Elder, Shantanu R. Jha, Jayameenakshi Venkatraman, Baptiste Royer, S. M. Girvin, Robert J. Schoelkopf, and Michel H. Devoret, Fast universal control of an oscillator with weak dispersive coupling to a qubit, Nat. Phys. **18**, 1464 (2022).
[22] Max Hofheinz, E. M. Weig, M. Ansmann, Radoslaw C. Bialczak, Erik Lucero, M. Neeley, A. D. O'Connell, H. Wang, John M. Martinis, and A. N. Cleland, Generation of Fock states in a superconducting quantum circuit, Nature (London) **454**, 310 (2008).
[23] Fabian Wolf, Chunyan Shi, Jan C. Heip, Manuel Gessner, Luca Pezzè, Augusto Smerzi, Marius Schulte, Klemens Hammerer, and Piet O. Schmidt, Motional Fock states for quantum enhanced amplitude and phase measurements with trapped ions, Nat. Commun. **10**, 2929 (2019).
[24] Erwin Schrödinger, Die gegenwärtige situation in der Quantenmechanik, Naturwissenschaften **23**, 844 (1935).
[25] Reinier W. Heeres, Philip Reinhold, Nissim Ofek, Luigi Frunzio, Liang Jiang, Michel H. Devoret, and Robert J. Schoelkopf, Implementing a universal gate set on a logical qubit encoded in an oscillator, Nat. Commun. **8**, 94 (2017).
[26] Nissim Ofek *et al.*, Extending the lifetime of a quantum bit with error correction in superconducting circuits, Nature (London) **536**, 441 (2016).
[27] L. Hu *et al.*, Quantum error correction and universal gate set operation on a binomial bosonic logical qubit, Nat. Phys. **15**, 503 (2019).
[28] P. Campagne-Ibarcq *et al.*, Quantum error correction of a qubit encoded in grid states of an oscillator, Nature (London) **584**, 368 (2020).
[29] K. M. Backes *et al.*, A quantum enhanced search for dark matter axions, Nature (London) **590**, 238 (2021).
[30] See Supplemental Material at http://link.aps.org/supplemental/10.1103/PhysRevLett.132.140801 for discussion of the dark photon interaction, experiment calibration, hidden Markov model, and dark matter exclusion calculations.
[31] J. R. Johansson, P. D. Nation, and Franco Nori, QuTiP: An open-source Python framework for the dynamics of open quantum systems, Comput. Phys. Commun. **183**, 1760 (2012).
[32] J. R. Johansson, P. D. Nation, and Franco Nori, QuTiP 2: A Python framework for the dynamics of open quantum systems, Comput. Phys. Commun. **184**, 1234 (2013).
[33] Srivatsan Chakram, Andrew E. Oriani, Ravi K. Naik, Akash V. Dixit, Kevin He, Ankur Agrawal, Hyeokshin Kwon, and David I. Schuster, Seamless high-Q microwave cavities for multimode circuit quantum electrodynamics, Phys. Rev. Lett. **127**, 107701 (2021).
[34] K. E. Cahill and R. J. Glauber, Density operators and quasiprobability distributions, Phys. Rev. **177**, 1882 (1969).
[35] Jens Koch, Terri M. Yu, Jay Gambetta, A. A. Houck, D. I. Schuster, J. Majer, Alexandre Blais, M. H. Devoret, S. M. Girvin, and R. J. Schoelkopf, Charge-insensitive qubit design derived from the Cooper pair box, Phys. Rev. A **76**, 042319 (2007).
[36] Vinay Ambegaokar and Alexis Baratoff, Tunneling between superconductors, Phys. Rev. Lett. **10**, 486 (1963).
[37] E. T. Jaynes and F. W. Cummings, Comparison of quantum and semiclassical radiation theories with application to the beam maser, Proc. IEEE **51**, 89 (1963).
[38] D. I. Schuster *et al.*, Resolving photon number states in a superconducting circuit, Nature (London) **445**, 515 (2007).
[39] M. Brune, S. Haroche, V. Lefevre, J. M. Raimond, and N. Zagury, Quantum nondemolition measurement of small photon numbers by Rydberg-atom phase-sensitive detection, Phys. Rev. Lett. **65**, 976 (1990).
[40] Sébastien Gleyzes, Stefan Kuhr, Christine Guerlin, Julien Bernu, Samuel Deléglise, Ulrich Busk Hoff, Michel Brune, Jean-Michel Raimond, and Serge Haroche, Quantum jumps of light recording the birth and death of a photon in a cavity, Nature (London) **446**, 297 (2007).
[41] Reinier W. Heeres, Brian Vlastakis, Eric Holland, Stefan Krastanov, Victor V. Albert, Luigi Frunzio, Liang Jiang, and Robert J. Schoelkopf, Cavity state manipulation using photon-number selective phase gates, Phys. Rev. Lett. **115**, 137002 (2015).
[42] H. Wang *et al.*, Measurement of the decay of Fock states in a superconducting quantum circuit, Phys. Rev. Lett. **101**, 240401 (2008).
[43] Nelson Leung, Mohamed Abdelhafez, Jens Koch, and David Schuster, Speedup for quantum optimal control from automatic differentiation based on graphics processing units, Phys. Rev. A **95**, 042318 (2017).
[44] Srivatsan Chakram, Kevin He, Akash V. Dixit, Andrew E. Oriani, Ravi K. Naik, Nelson Leung, Hyeokshin Kwon, Wen-Long Ma, Liang Jiang, and David I. Schuster, Multimode photon blockade, Nat. Phys. **18**, 879 (2022).
[45] Navin Khaneja, Timo Reiss, Cindie Kehlet, Thomas Schulte-Herbrüggen, and Steffen J. Glaser, Optimal control of coupled spin dynamics: Design of NMR pulse sequences by gradient ascent algorithms, J. Magn. Reson. **172**, 296 (2005).
[46] Wayne M. Itano, D. J. Heinzen, J. J. Bollinger, and D. J. Wineland, Quantum Zeno effect, Phys. Rev. A **41**, 2295 (1990).
[47] Huaixiu Zheng *et al.*, Accelerating dark-matter axion searches with quantum measurement technology, arXiv:1607.02529.
[48] F. A. M. de Oliveira, M. S. Kim, P. L. Knight, and V. Bužek, Properties of displaced number states, Phys. Rev. A **41**, 2645 (1990).
[49] L. Sun *et al.*, Tracking photon jumps with repeated quantum non-demolition parity measurements, Nature (London) **511**, 444 (2014).
[50] Joshua W. Foster, Nicholas L. Rodd, and Benjamin R. Safdi, Revealing the dark matter halo with axion direct detection, Phys. Rev. D **97**, 123006 (2018).

[51] Samuel D. McDermott and Samuel J. Witte, Cosmological evolution of light dark photon dark matter, Phys. Rev. D **101**, 063030 (2020).

[52] Ofir Milul, Barkay Guttel, Uri Goldblatt, Sergey Hazanov, Lalit M. Joshi, Daniel Chausovsky, Nitzan Kahn, Engin Çiftyürek, Fabien Lafont, and Serge Rosenblum, Superconducting cavity qubit with tens of milliseconds single-photon coherence time, PRX Quantum **4**, 030336 (2023).

[53] K. Wurtz, B. M. Brubaker, Y. Jiang, E. P. Ruddy, D. A. Palken, and K. W. Lehnert, Cavity entanglement and state swapping to accelerate the search for axion dark matter, PRX Quantum **2**, 040350 (2021).